



**Kinetic Modeling and Mechanistic Investigations of
Transesterification of Propylene Carbonate with Methanol
over Fe-Mn Double Metal Cyanide Catalyst**

Journal:	<i>Reaction Chemistry & Engineering</i>
Manuscript ID	RE-ART-09-2019-000372.R1
Article Type:	Paper
Date Submitted by the Author:	21-Oct-2019
Complete List of Authors:	Song, Ziwei; Yanshan University, Subramaniam, Bala; University of Kansas, Center for Environmentally Beneficial Catalysis Chaudhari, Raghunath; University of Kansas, Chemical & Petroleum Engineering

Kinetic Modeling and Mechanistic Investigations of Transesterification of Propylene Carbonate with Methanol over Fe-Mn Double Metal Cyanide Catalyst

Ziwei Song,^{a,b,c} Bala Subramaniam,^{a,b} and Raghunath V. Chaudhari*^{a,b}

^aCenter for Environmentally Beneficial Catalysis, University of Kansas, 1501 Wakarusa Dr. Lawrence, KS 66047, United States

^bDepartment of Chemical & Petroleum Engineering, University of Kansas, 1503 W 15th St. Lawrence, KS 66045, United States

^cDepartment of Chemical Engineering, College of Environmental and Chemical Engineering, Yanshan University, Qinhuangdao 066004, China

*Corresponding author: rvc1948@ku.edu

KEYWORDS: double metal cyanide, transesterification, dimethyl carbonate,

microkinetic modeling

Abstract

Kinetic modeling of transesterification of propylene carbonate with methanol using Fe-Mn double metal cyanide catalyst has been investigated based on experimental data obtained under kinetically controlled conditions in a batch slurry reactor in the 140-200 °C range. A simple two-step power law model was found to represent the experimental data well. In addition, a detailed kinetic model based on a molecular level description of the reaction mechanism is also evaluated to provide better insight into the reaction mechanism. It is found that a kinetic model based on the following mechanistic steps provides the best description of the experimental data: (a) activation of methanol by the catalyst to form a methoxy intermediate, (b) activation of propylene carbonate by interaction with the methoxy intermediate to form a second intermediate, (c) reaction of the second intermediate with methoxy species to form a third intermediate which decomposes into the final products dimethyl carbonate and propylene glycol with regeneration of the catalyst precursor. The kinetic model along with mechanistic insights from the present study provide rational guidance for catalyst redesign and process optimization.

INTRODUCTION

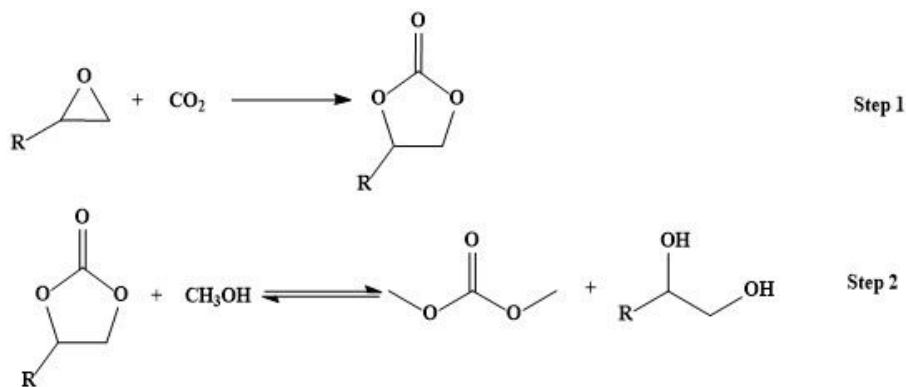
Various strategies for CO₂ utilization have attracted significant interest in the last decade, including catalytic conversion of CO₂ to value added chemicals and fuels.¹⁻⁵ CO₂ can be catalytically converted to various important industrial products, such as hydrocarbons, cyclic carbonates,⁶⁻⁹ organic carbonates,¹⁰⁻¹¹ carboxylic acids¹²⁻¹³ as well as fuel range compounds including methane, methanol.¹⁴

Dimethyl carbonate (DMC), is an environmentally benign substitute for phosgene, dimethyl sulfate and methyl halide, and can be produced through a two-step process using CO₂ as a starting material (Scheme 1).¹⁵⁻¹⁶ Transesterification of cyclic carbonate with methanol has drawn much attention as a phosgene-free process for making DMC.

Previous studies have focused on the development of various catalysts for the transesterification of cyclic carbonates with methanol, including sodium methoxide¹⁷, alkali metals¹⁸, basic metal oxides^{15, 19-20}, ion exchange resins²¹, and hydrotalcites²². Although homogeneous catalysts display high activity under mild reaction conditions,¹⁷ a major drawback is the usual difficulty in separation and recovery of products and catalysts. Therefore, the development of heterogeneous catalysts for transesterification continues to attract research interest.

In 1960s, the General Tire & Rubber Company discovered double metal cyanide complex has high activity for the ring-opening polymerization of epoxy compounds, cyclic anhydrides and cyclic sulfides²³. Ever since then, companies like Arco Chemical Technology²⁴, the Dow Chemical Company²⁵, Shell Oil Company²⁶ have put huge effort into the development of this type of catalysts. Till now, this kind of catalysts has been

successfully used industrially in various ring-opening reactions, such as in epoxide polymerization reactions,²⁷ and copolymerization reaction of epoxide with CO₂.²⁷⁻³³ Recently, Fe-Zn double metal cyanide catalyst has been successfully used in transesterification reaction for the manufacture of biodiesel.³⁴ Additionally, Srivastava and coworkers have found Fe-Zn to be an excellent heterogeneous catalyst for transesterification of propylene carbonate with methanol.³⁵ However, the cited reports focus on the structural properties of different double metal cyanides along with activity testing with very little information on the kinetics and reaction engineering aspects, which are essential for rational process development. Although several reports have provided insights into the possible mode of activation of cyclic carbonate and methanol on metal catalysts,³⁵⁻³⁶ there is a lack of reliable information on the mechanistic and kinetic aspects of heterogeneously catalyzed transesterification of cyclic carbonate.



Scheme 1 Reaction scheme for production of dimethyl carbonate from CO₂

In our previous work, we reported that Fe-Mn double metal cyanide complex shows a significantly higher activity for the transesterification of cyclic carbonates with methanol compared with other double metal cyanide complexes³⁷. In this work, detailed kinetic modeling of the transesterification of propylene carbonate (PC) with methanol over Fe-Mn double metal cyanide is reported. The effects of several experimental parameters, including temperature (140-200 °C), PC initial concentration (1.1-4.3 kmol/m³), and initial methanol

concentration (1.2-4.8 kmol/m³) on the intrinsic conversion and product formation profiles were studied. The data were analyzed with empirical power law models as well as detailed kinetic models based on molecular description of the various reaction steps of the proposed mechanisms. A kinetic model involving sequential activation of reactants and intermediates with catalyst was found to best represent the experimental data. The results have thus provided better insights into the reaction mechanism and kinetics of this industrially important reaction system.

EXPERIMENTAL

Materials

Chemicals such as methanol (99.9%), PC (99.7%), DMC (extra dry, 98+%), propylene glycol (PG, 99.5+%) and mesitylene (98%) were purchased from Sigma-Aldrich. K₄Fe(CN)₆·3H₂O (98%) were obtained from Alfa Aesar. All chemicals were used as received without further treatment. The Fe-Mn double metal cyanide catalysts were prepared using the method described in previous work.³⁵

Reactor Setup and Procedures

The kinetic experiments were conducted in a stirred slurry reactor (Parr reactor). The reactor system consists of a 300 mL reactor equipped with a thermocouple, pressure transducer, gas inlet and stirring impeller. The temperature, pressure and stirring speed are independently controlled and monitored with Labview® software through the control module of the reactor system. In a typical reaction experiment, a methanol-based slurry was charged in the autoclave with a known amount of catalyst and mesitylene (internal standard). The reactor was sealed and loaded into the setup. Following this step, 0.69 MPa N₂ gas was introduced into the reactor while stirring slowly (~50 rpm). The mixture was then heated to the desired temperature, after which another reactant, PC, was pumped into the reactor using a HPLC

pump [Scientific Systems, Inc. (SSI) Series I pump] to the desired initial concentration. After the mixture reaches the desired temperature, the reaction was initiated by increasing the stirrer speed to 1000 rpm. During the reaction, liquid samples were withdrawn at different times to develop concentration-time profiles for the reactants and products. The liquid samples were analyzed using GC analysis (GC-7860A) equipped with ZB-FFAP capillary column of 30 m length and a flame-ionization detector (FID), the detail information is shown in Supporting Information Part 2.

RESULTS AND DISCUSSION

Reaction Kinetics

Detailed kinetic models for PC transesterification were investigated using experimentally measured concentration-time profiles at different temperatures and different reaction conditions (Figure 1). These profiles capture the temporal evolution of various products including intermediates. Typical experiment was repeated twice and values of substrate/product concentration were measured (see Figure S3 in Supporting Information). The standard deviation was 3.92%.

Concentration-time profiles. It is clear from the concentration-time profiles that the major products are DMC and PG, with a smaller but significant amount of the mono transesterified product, 2-hydroxypropyl methyl carbonate (2-HMC). At 140 °C (Figure 1 a), the concentration of reactant PC decreased from 1.1 kmol/m³ to 0.56 kmol/m³ in 3 h. Concentrations of DMC and PG increased gradually with reaction time, while the formation of 2-HMC first increased and then decreased to nearly none. As expected, when the temperature is increased from 140 °C to 200 °C, the formation rates of products show a significant increase. The various temporal reaction profiles are provided in the Supporting Information (Part 3, Figures S3-S6). Data from sixteen temporal profiles at four different

temperatures were used for model discrimination and parameter estimation.

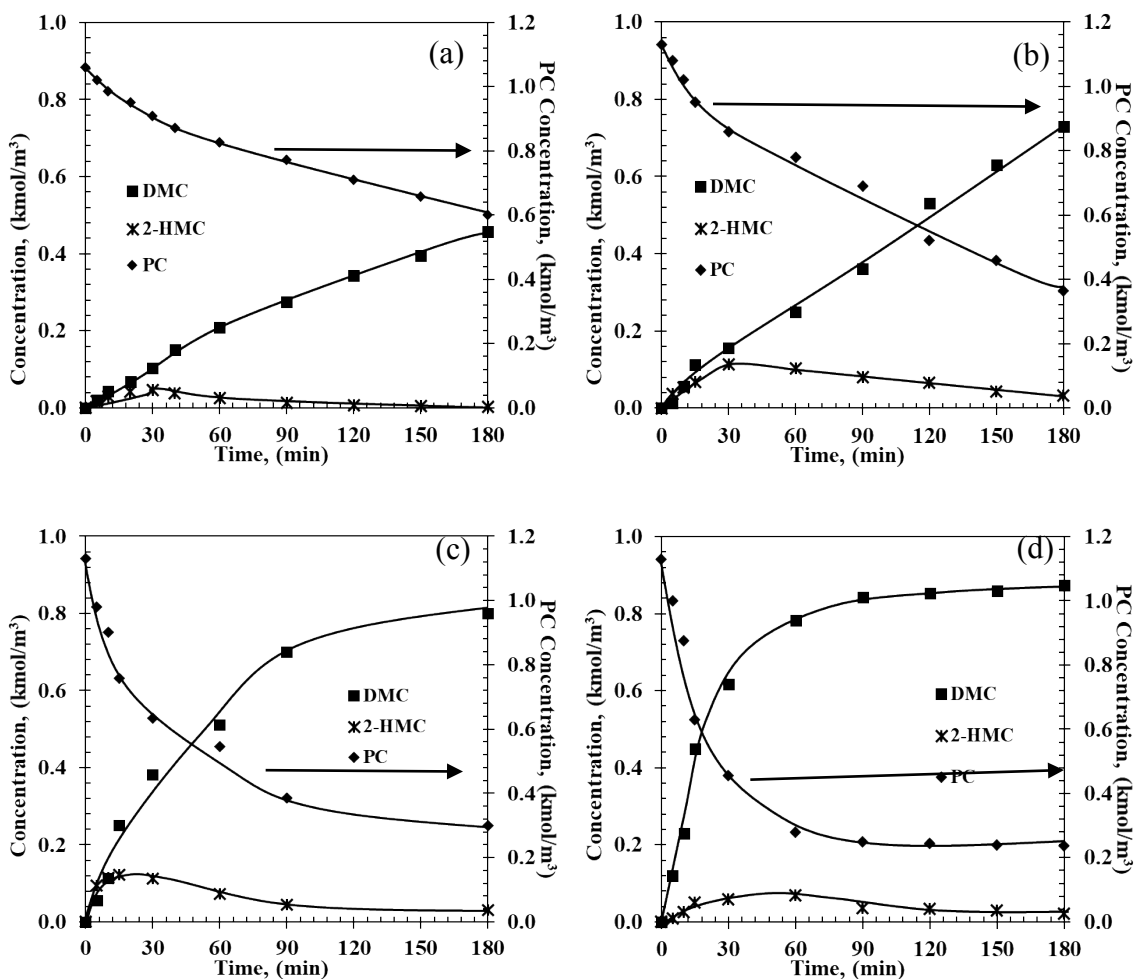


Figure 1 Temporal concentration-time profiles of PC conversion over Fe-Mn catalyst at (a) 140 °C; (b) 160 °C; (c) 180 °C; (d) 200 °C. Reaction conditions: PC: 1.1 kmol/m³; methanol: 22.2 kmol/m³; catalyst: 5 kg/m³; 0.69 MPa initial N₂.

Analysis of mass transfer effects. Since transesterification reaction involves a liquid-solid catalytic reaction, liquid-solid and intraparticle mass transfer limitations for the limiting reactant, PC were considered (since methanol is in large excess). To assess these limitations, the criteria described by Ramachandran and Chaudhari were used.³⁸ In these criteria, experimentally measured rates were compared with maximum rates of the mass transfer steps liquid-solid and intraparticle mass transfer steps. Details of calculations for a few cases are shown in the Supporting Information (Part 5). The analysis showed that both liquid-solid and intraparticle mass transfer limitations were negligible confirming that the experimental

data were obtained in the kinetic regime.

Effect of Initial Substrates Concentration: The effect of initial substrate (PC) concentration on initial reaction rates is shown in Figure 2 a. As PC concentration increased from 1.1 to 4.3 kmol/m³, the initial reaction rate increased from 0.65 (10⁻²) to 2.32 (10⁻²) kmol/(m³·min) at 140 °C suggesting first-order dependence of the initial reaction rate with PC concentration. Similar trends were also observed at the higher reaction rates observed at 160 °C, 180 °C and 200 °C. The effect of methanol concentration on initial reaction rate shows a similar trend at 200 °C (Figure 2 b).

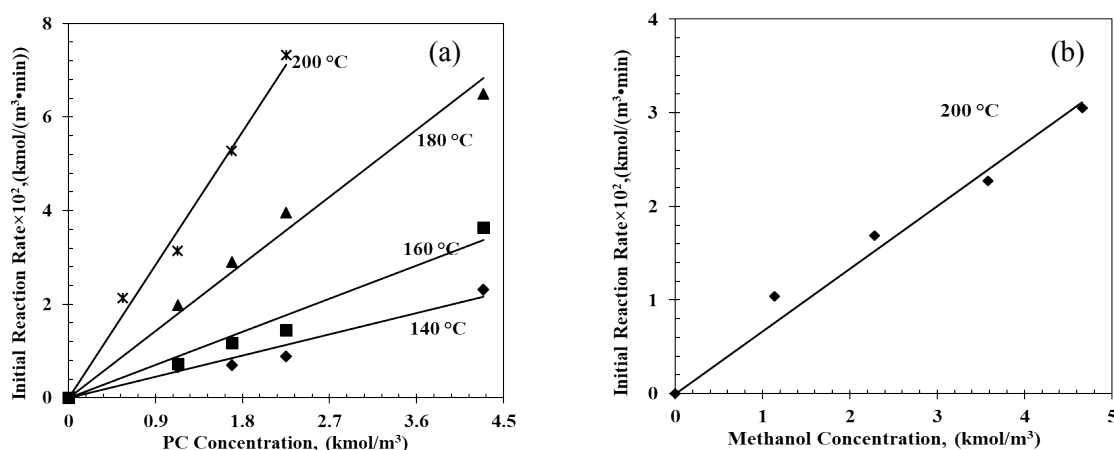
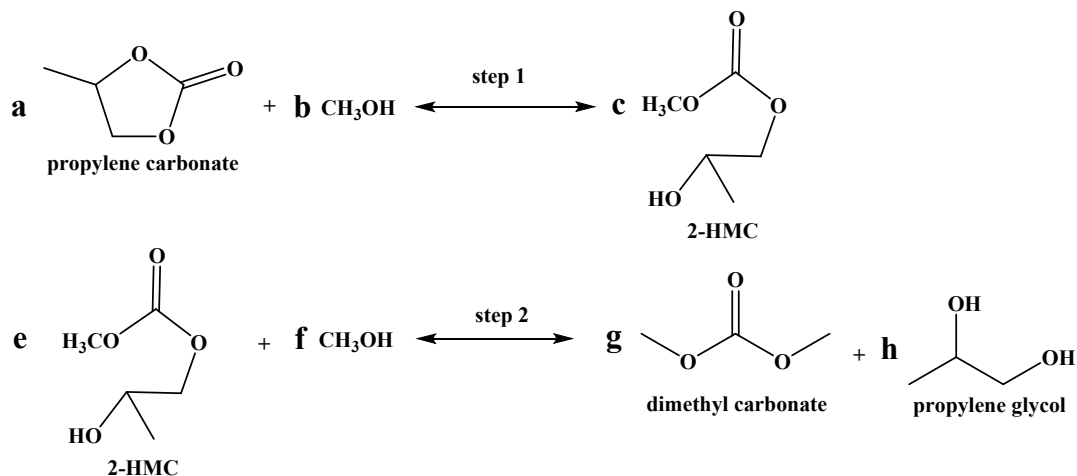


Figure 2 Effects of (a) PC initial concentration and (b) methanol initial concentration on initial reaction rates. Reaction conditions: (a) methanol, 17.9-22.8 kmol/m³; catalyst, 5 kg/m³; T=140 °C; 0.69 MPa N₂; (b) PC, 9.3-10.8 kmol/m³; catalyst, 5 kg/m³; T=200 °C; 0.69 MPa N₂

Apparent activation energy. The estimated first-order forward reaction rate constants for PC transesterification at 140 °C, 160 °C, 180 °C and 200 °C, estimated from the slopes of the regression line in Figure 2 a, were 0.50 min⁻¹, 0.79 min⁻¹, 1.60 min⁻¹ and 3.17 min⁻¹, respectively. The activation energy was estimated as 50.4 kJ/mol, with a pre-exponential factor of 1.07 (10⁴) min⁻¹ (See Figure S7 in Supporting Information).

Two-step power law model. Given that a significant amount of intermediate 2-HMC was formed during the reaction, the following reaction scheme (Scheme 2) was considered for

the power law model. Since the initial reaction rate is first order in both PC and methanol concentration, the exponents a and b are fixed at a value of unity ($a=b=1$). The rate expressions and batch reactor mass balance equations of each component are given by Equations (1)-(7).



Scheme 2 Two-step reaction scheme

$$r_1 = k_1 C_{PC} C_{MeOH} - k_{-1} C_{2-HMC}^c \quad (1)$$

$$r_2 = k_2 C_{2-HMC}^e C_{MeOH}^f - k_{-2} C_{DMC}^g C_{PG}^h \quad (2)$$

$$\frac{d[PC]}{dt} = -\omega r_1 \quad (3)$$

$$\frac{d[MeOH]}{dt} = -\omega(r_1 + fr_2) \quad (4)$$

$$\frac{d[DMC]}{dt} = \omega gr_2 \quad (5)$$

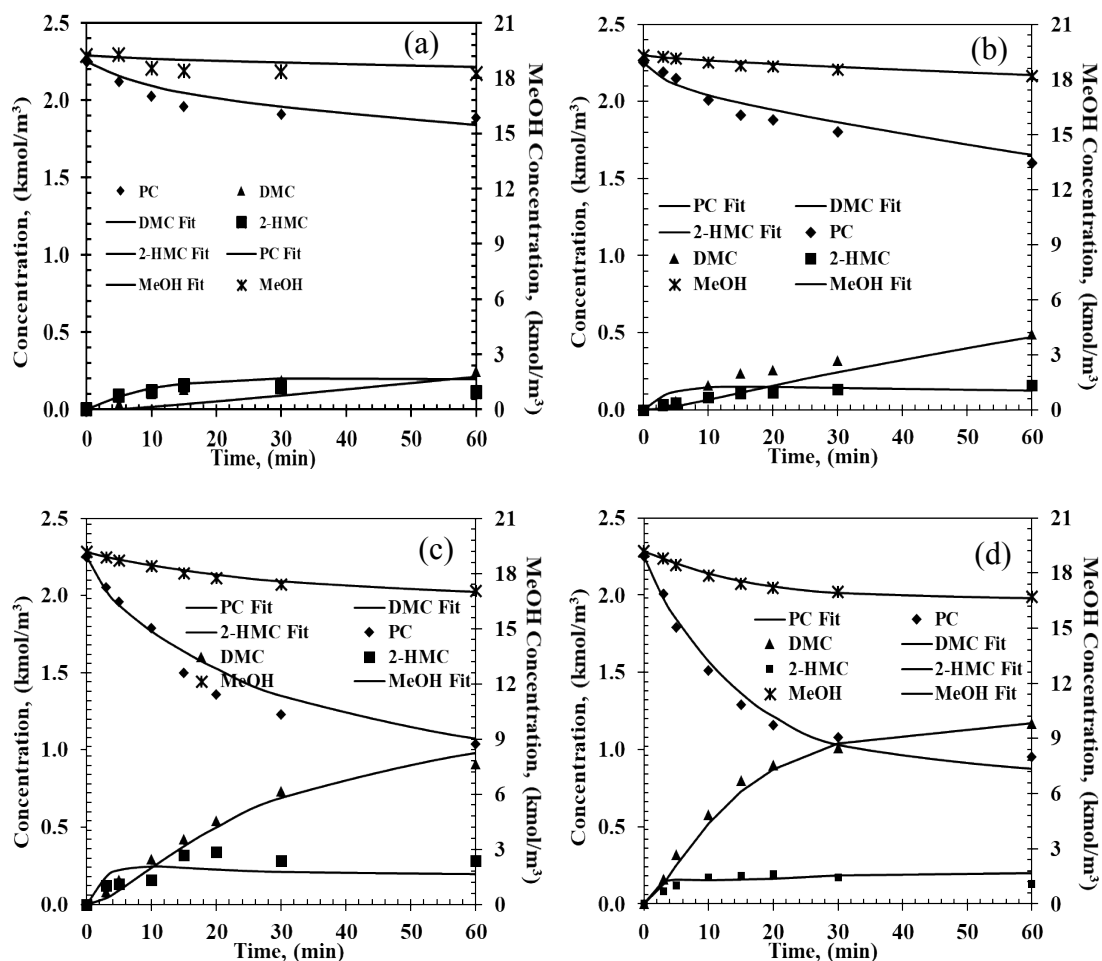
$$\frac{d[PG]}{dt} = \omega hr_2 \quad (6)$$

$$\frac{d[2HMC]}{dt} = \omega(cr_1 - er_2) \quad (7)$$

Where, r_1 and r_2 are specific reaction rates for step 1 and step 2, k_1 , k_{-1} and k_2 , k_{-2} are temperature dependent forward and reversible reaction rate constants for step 1 and step 2, respectively, and ω is the catalyst concentration.

To simulate the experimental concentration-time data, Equations (1)-(7) were solved with

an optimization routine using Athena Visual Studio software³⁹⁻⁴². For the parameter estimation and model discrimination, several convergence criteria were used, as summarized in the Supporting Information (Part 7). Through the parameter estimation, it is found that when $c=d=e=f=g=h=1$, the power law fits the experimental data well. Typical results of experimental and predicted concentration-time profiles for various chemical components are shown in Figure 3.



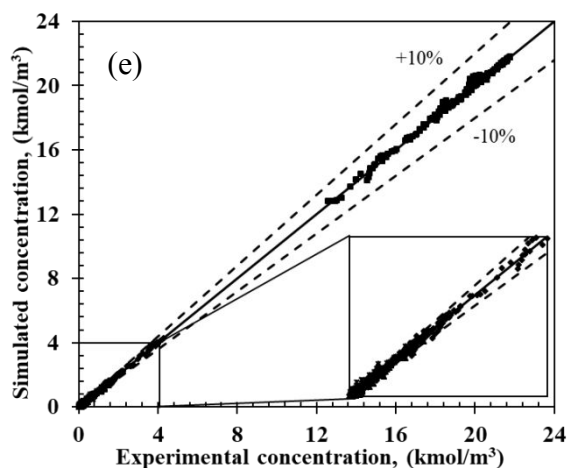


Figure 3 Experimental and predicted concentration-time profiles from two-step power law. Reaction conditions: PC, 2.25 kmol/m³; methanol, 20.5 kmol/m³; catalyst, 5 kg/m³; 0.69 MPa N₂. (a) 140 °C, (b) 160 °C, (c) 180 °C, (d) 200 °C, (e) Parity plot of the simulated and experimental concentrations for the four chemicals. Markers: experimental values; lines: estimated values from power law

A similar procedure was followed for modeling the data from all the 16 experiments at four different temperatures. As shown in Figure 3 e, the predicted rates are well within $\pm 10\%$ of the experimental rates demonstrating that the empirical power law model can be applied to predict the temporal concentration-time profiles for reactor design and optimization in the range of the experimental conditions studied.

Optimized values of the rate parameters are shown in Arrhenius plot in Figure S8 while the reaction rate constants and activation energies are presented in Table 1. An activation energy of 47.0 ± 20.2 kJ/mol was observed for the ring opening reaction, the mono-transesterification of PC with methanol using Fe-Mn catalyst. In contrast, a much higher activation energy (79.6 ± 9.8 kJ/mol) was observed for the second step transesterification of 2-HMC with methanol. The higher energy barrier of the second step is attributed to the release of ring strain energy when the ring of PC was broken.⁴³

Table 1 Values of activation energy and rate constants derived from power law

Rate Constants	140 °C ^a	160 °C ^a	180 °C ^a	200 °C ^a	E _a ^b
----------------	---------------------	---------------------	---------------------	---------------------	-----------------------------

$k_1 \times 10^1, (\text{m}^6 \cdot \text{min}^{-1} \cdot \text{kmol}^{-2})$	1.26±0.47	2.42±0.57	5.50±0.61	6.52±0.59	47.0±20.2
$k_{-1} \times 10^{-1}, (\text{m}^3 \cdot \text{min}^{-1} \cdot \text{kmol}^{-1})$	1.76±0.88	4.64±1.47	4.49±0.63	4.57±0.72	23.7±27.2
$k_2, (\text{m}^6 \cdot \text{min}^{-1} \cdot \text{kmol}^{-2})$	0.26±0.024	0.78±0.049	1.60±0.12	5.38±0.97	79.6±9.8
$k_{-2}, (\text{m}^6 \cdot \text{min}^{-1} \cdot \text{kmol}^{-2})$	0.28±0.06	0.60±0.16	4.29±0.43	12.9±2.89	108.9±14.6

^a Rate constants with 95% confidence level

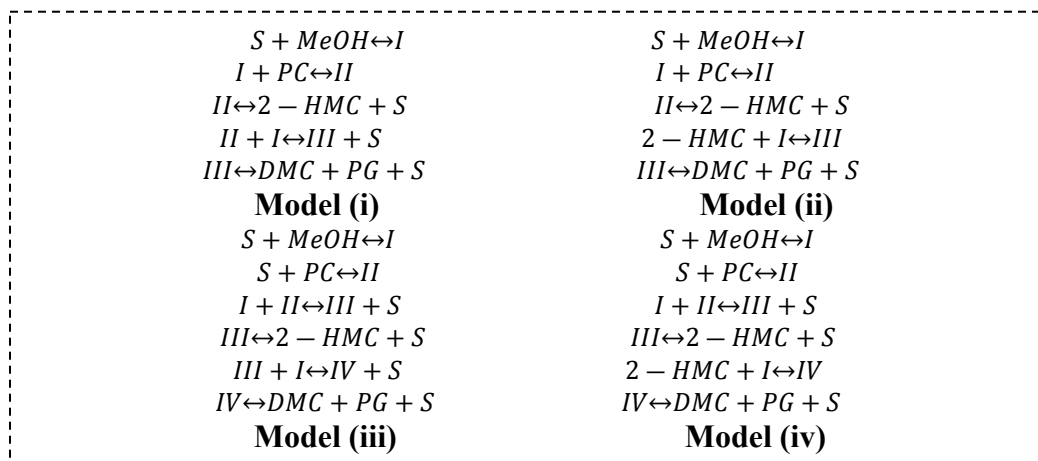
^b Unite of E_a : kJ/mol, detailed error analysis is in Supporting Information.

Mechanistic Modelling

Reaction Mechanism and Proposed Models. Transesterification reaction between cyclic carbonates and methanol generally follows the following main steps: 1) the formation of M-O-CH_3 intermediate through the interaction between CH_3O^- from methanol and metal active center⁴⁴⁻⁴⁶, 2) the formation of mono-transesterified product (2-HMC and 1-HP-2-MC) from activated methanol with PC or with activated PC^{36, 47-51}; 3) further transesterification of mono-transesterified product/activated mono-transesterified product with activated methanol to form the final product DMC and PG. However, a specific activation sequence of methanol, PC and 2-HMC is not obvious from the general trends observed.

In our previous work, we found that Mn is the active species while Fe functions as a metal-dispersing agent and a stabilizer of the cyano-bridged complex ensuring a truly heterogeneous catalyst.^{35, 37} Additionally, based on the reaction orders estimated from the power law model, it is clear that the reaction rate shows a first order dependent on PC, methanol, 2-HMC, DMC and PG concentrations. Furthermore, from our previous FTIR test,³⁷ PC is known to be adsorbed on the catalyst. However, it is unclear whether PC is adsorbed on the catalyst directly or on an active intermediate. To better understand the reaction activation sequence and the overall mechanism, four kinetic models were evaluated

(Scheme 3) based on different sequential reaction steps. The possible catalytic cycles are shown in Scheme 5 a. Each model was fitted with all the experimental data and discriminated based on the predictive ability of the models and the whether the values of the regressed reaction parameters make physical sense.



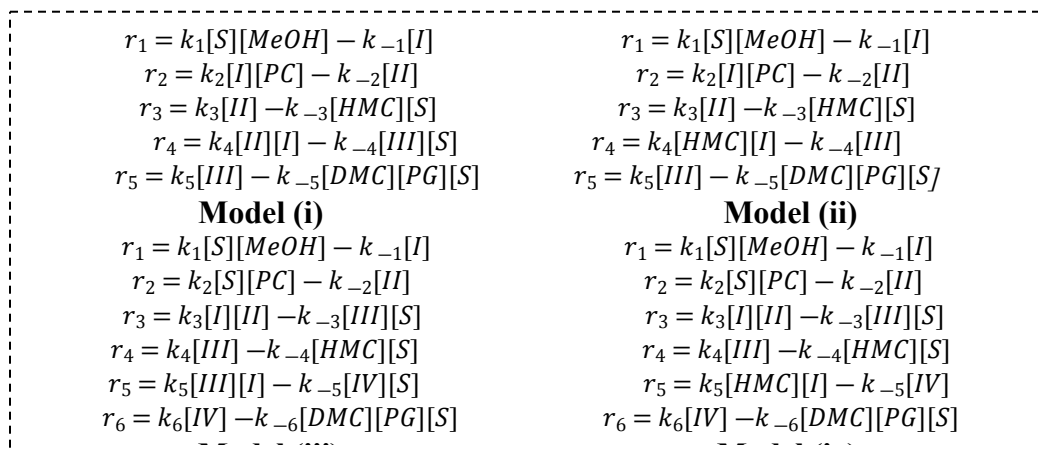
Scheme 3. Proposed kinetic models for transesterification of PC with methanol on Fe-Mn catalyst

For model (i), methanol is first activated by Fe-Mn complex (S stands for the active sites) to form the intermediate I.^{30, 35} Then, PC reacts with intermediate I to form intermediate II,^{30, 35} followed by decomposition of intermediate II into the mono-transesterified product, 2-HMC, while releasing the catalytic site for further reaction. Further, intermediate II reacts with another activated methanol (intermediate I) to form intermediate III followed by decomposition into product DMC and PG. The only difference between model (ii) and model (i) is in step (4), where 2-HMC is assumed to react with activated methanol (intermediate I).

For model (iii), methanol is first activated by Fe-Mn complex to form the intermediate I;^{30, 35} simultaneously, PC is activated to form intermediate II²⁰. Then, intermediates I and II react to form intermediate III followed by its decomposition into mono-transesterified product 2-HMC and catalyst. Intermediate III further reacts with another activated methanol (intermediate I) species to form intermediate IV which decomposes into the products DMC and PG. The only difference between model (iv) and model (iii) is in step (5), where the 2-

HMC is assumed to react with activated methanol (intermediate I).

Rate Equations and Batch Reactor Equations. The rate equations for each of the individual steps of the four models are summarized in Scheme 4. The corresponding batch reactor model equations are summarized in Table S1 in Supporting Information.



Scheme 4. Rate equations for various steps in each model

For all the four kinetic models, no specific step was assumed as rate-determining, which allows the evaluation of rate parameters for each reaction step including those involving catalytic intermediate species.

The initial conditions are:

at $t=0$, $[PC]=[PC]_0$, $[MeOH]=[MeOH]_0$, $[DMC]=[PG]=[2-HMC]=0$, $[S]=C_0$, $[I]=[II]=[III]=[IV]=0$,

where, $[PC]_0$, $[MeOH]_0$, C_0 represent the initial concentrations of PC, methanol and catalyst precursor, respectively. For solving these ODEs, reasonable initial guesses were provided for the rate constants with ranges determined from the power law model. The ODEs were solved using Athena Visual Studio. Identical convergence criteria and constraints were used as those used in the power law models.

Model validation. To show the feasibility of the mechanistic model for the description of the transesterification of PC with methanol developed above, an additional set of data was used

to compare with predictions by the model. The operating conditions of this experiment were differed from other experiments in this work used for fitting parameters. The aim of this experiment was to demonstrate that Model (i) can be used to predict concentration-time profiles over wider range of conditions. Figure 4 illustrates temporal concentration-time profiles for the additional experiment, with the symbols representing the experimental results and lines representing the predicted results using Model (i). A comparison between the experimental and predicted data indicates a high accuracy of Model (i).

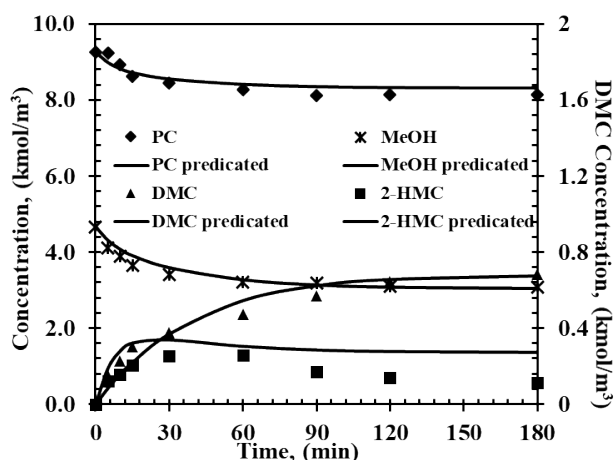


Figure 4 Experimental and predicted concentration-time profiles for the validation experiment.

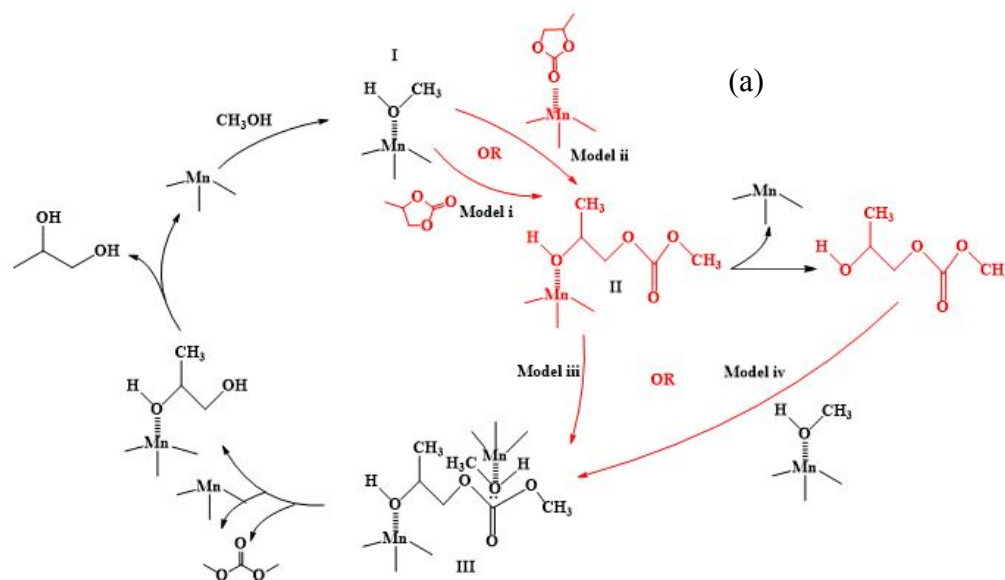
Reaction conditions: $T=200\text{ }^{\circ}\text{C}$, PC, 9.8 kmol/m^3 ; methanol, 3.58 kmol/m^3 ; catalyst, 5 kg/m^3 ; 0.69 MPa N_2 .

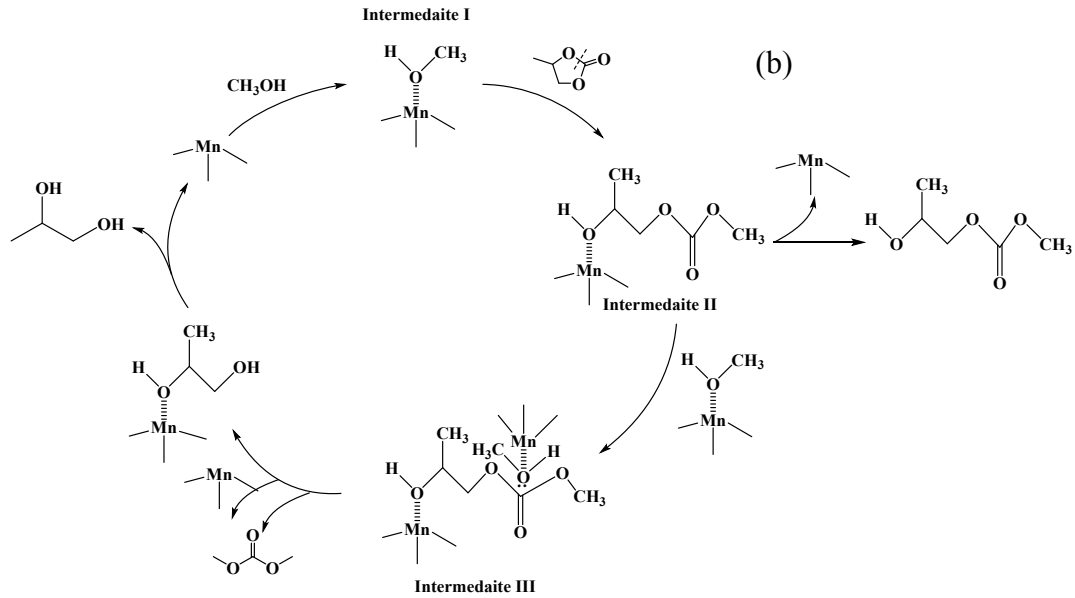
Proposed Mechanism Based on Model Discrimination. The main observations of the data regression using models (i)–(iv) are summarized in Table 2. The estimated parameters are shown in Table 4 [for model (i)] and in the Supporting Information Tables S1-S3 [for models (ii)–(iv)]. Model (i) parameters were deemed to be acceptable based not only on the quality of fit with the experimental data but also on realistic parameter values. As summarized in Table 3, the fit with other models yielded parameter values whose signs and /or magnitudes cannot be reconciled with typical values for these parameters.

Table 2 Basis for Discrimination of Models (i)-(iv)

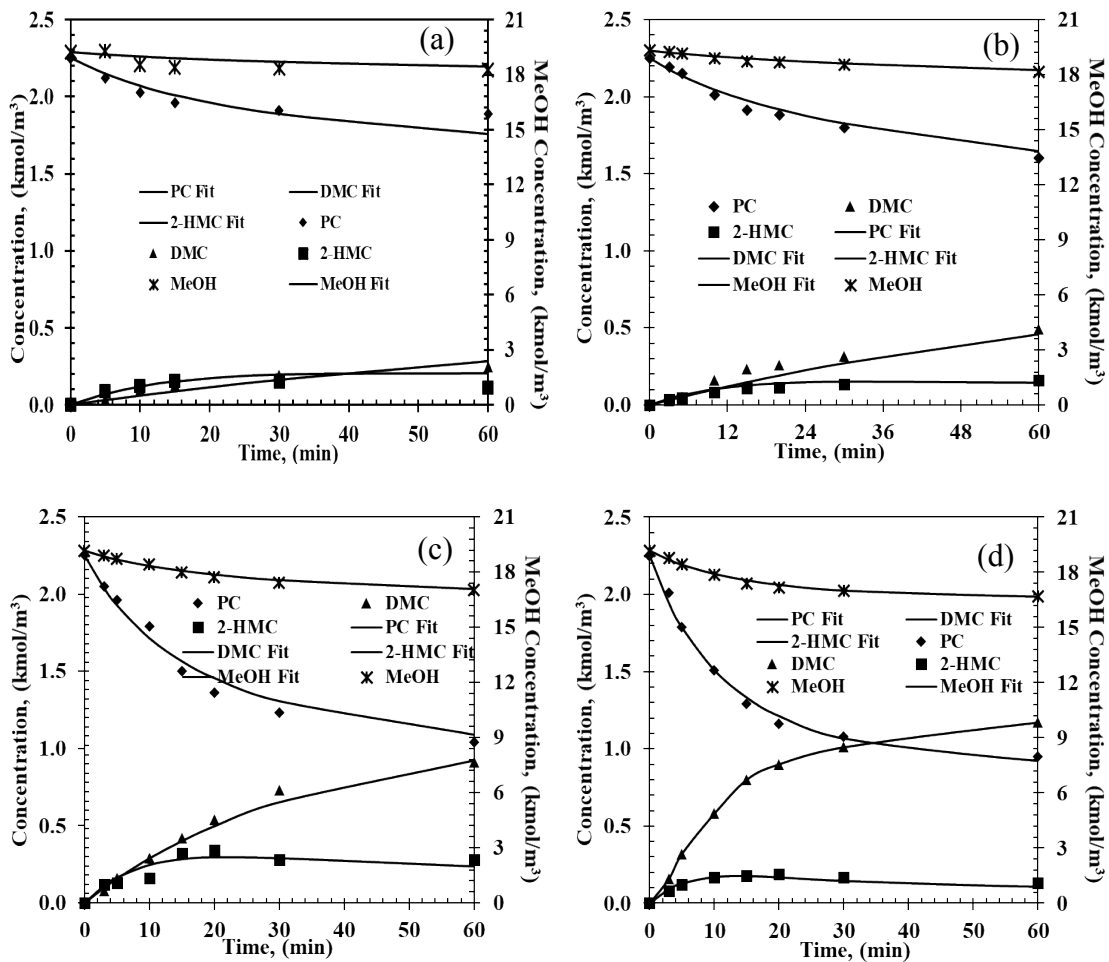
Models	Model Discrimination Basis
Model i	Best fit with experimental data
Model ii	Rate constants (k_{-3} and k_{-4}) decrease with increasing temperature, and 95% confidence level > 120% for k_2 and k_{-2}
Model iii	Negative k_{-1} at 160 °C, the constants do not agree with Arrhenius Equation
Model iv	95% confidence level > 120% for k_4 at 160 °C, activation energy of step 4 > 400 kJ/mol

A schematic description of the mechanism represented in Model (i) is presented in Scheme 5 b as a complete catalytic cycle. The kinetic parameters obtained from fitting Model (i) with experimental data are listed in Table 3. The activation energy values for each step are estimated from the Arrhenius Equations (Supporting Information Figure S9). Additionally, a comparison of predicted and experimental data at different temperatures is also shown in Figure . The excellent match between the experimental and predicted results at various reaction conditions indicates that the proposed reaction mechanism in Scheme 5 represents the transesterification of PC and methanol satisfactorily.





Scheme 5. a Possible activation sequences in a catalytic cycle, b Proposed reaction mechanism based on model discrimination



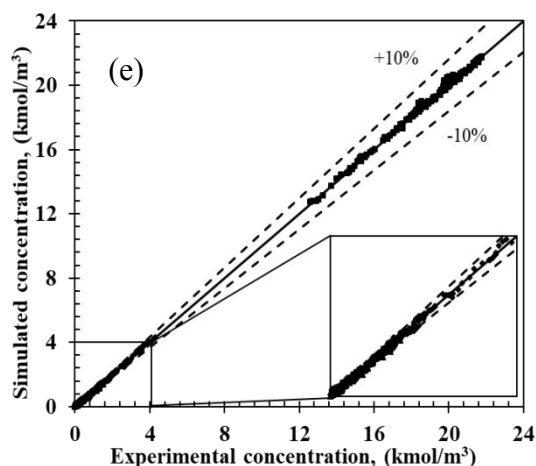


Figure 5 Experimental and predicted concentration-time profiles from the micro kinetic model. Reaction conditions: PC, 2.25 kmol/m³; methanol, 20.5 kmol/m³; catalyst, 5 kg/m³; 0.69 MPa N₂. (a) 140 °C, (b) 160 °C, (c) 180 °C, (d) 200 °C, (e) parity plot

Table 3 Rate constants and activation energy for each reaction step

Rate Constants	140 °C ^a	160 °C ^a	180 °C ^a	200 °C ^a	E _a ^b
k ₁ ×10 ⁻² , (m ³ ·min ⁻¹ ·kmol ⁻¹)	0.51±0.01	1.22±0.06	2.79±0.06	4.81±0.11	61.7±2.7
k ₋₁ ×10 ⁻⁴ , (min ⁻¹)	2.15±0.31	5.11±0.20	8.15±0.52	14.0±1.04	49.6±7.8
k ₂ ×10 ⁻⁴ , (m ³ ·min ⁻¹ ·kmol ⁻¹)	2.80±0.26	7.18±0.27	1.24±0.82	17.20±0.85	49.1±5.1
k ₋₂ ×10 ⁻⁶ , (min ⁻¹)	0.48±0.10	2.11±0.06	4.28±0.50	6.26±0.17	68.8±11.3
k ₃ ×10 ⁻² , (min ⁻¹)	1.21±0.10	2.56±0.04	8.13±1.25	9.50±0.70	60.0±8.4
k ₋₃ , (m ³ ·min ⁻¹ ·kmol ⁻¹)	2.32±0.19	3.98±0.69	6.85±1.36	8.34±0.67	35.8±10.8
k ₄ ×10 ⁻⁵ , (m ³ ·min ⁻¹ ·kmol ⁻¹)	1.84±0.25	5.06±1.30	8.17±0.46	16.80±2.39	58.0±13.9
k ₋₄ ×10 ⁻⁴ , (m ³ ·min ⁻¹ ·kmol ⁻¹)	0.68±0.20	1.66±1.36	1.99±0.33	2.48±0.39	33.4±44.2
k ₅ ×10 ⁻³ , (min ⁻¹)	0.23±0.06	0.90±0.21	2.96±0.48	5.16±0.68	86.2±14.8
k ₋₅ , (m ⁶ ·kmol ⁻² ·min ⁻¹)	3.17±0.62	8.23±5.67	9.20±1.59	18.68±2.78	44.29±37.3

^a Rate constants with 95% confidence level

^b Unit of E_a: kJ/mol, the detail error calculation is in Supporting Information.

CONCLUSION

A detailed kinetic study for transesterification of PC with methanol using Fe-Mn double metal cyanide revealed that both a two-step empirical power law model and a mechanistic model based on transesterification mechanism were found to fit the experimental data well.

Four mechanistic models based on different activation sequence of methanol, PC and 2-HMC were also considered. Through model discrimination based on the quality of fit between experimental and model-predicted data as well as the realism of the parameter values, it was concluded that methanol was first activated by the catalyst to form intermediate I, which then reacts with PC to form intermediate II. Next, the intermediate II reacts with activated methanol (intermediate I) to form intermediate III, which decomposed into to DMC and PG, the major products. These results provide valuable insights into the reaction pathways underlying transesterification. The kinetic model is useful for rational reactor design and further optimization of this industrially significant reaction system.

AUTHOR INFORMATION

Corresponding author

*Raghunath V. Chaudhari. E-mail: rvc1948@ku.edu

Notes

The authors declare no competing financial interest.

ACKNOWLEDGEMENT

The authors gratefully acknowledge support to this work from National Science Foundation and Environmental Protection Agency Grant, NSF-EPA 1339661.

REFERENCE

1. Darensbourg, D. J., Chemistry of Carbon Dioxide Relevant to Its Utilization: A Personal Perspective. *Inorganic Chemistry* **2010**, *49* (23), 10765-10780.
2. Song, C., Global challenges and strategies for control, conversion and utilization of CO₂ for sustainable development involving energy, catalysis, adsorption and chemical processing. *Catalysis today* **2006**, *115* (1-4), 2-32.
3. Aresta, M., *Carbon dioxide as chemical feedstock*. John Wiley & Sons: 2010.
4. Aresta, M.; Dibenedetto, A.; Angelini, A., Catalysis for the valorization of exhaust carbon: from CO₂ to chemicals, materials, and fuels. Technological use of CO₂. *Chemical reviews* **2013**,

114 (3), 1709-1742.

5. Omae, I., Recent developments in carbon dioxide utilization for the production of organic chemicals. *Coordination Chemistry Reviews* **2012**, 256 (13-14), 1384-1405.
6. Sun, J.; Zhang, S.; Cheng, W.; Ren, J., Hydroxyl-functionalized ionic liquid: a novel efficient catalyst for chemical fixation of CO₂ to cyclic carbonate. *Tetrahedron Letters* **2008**, 49 (22), 3588-3591.
7. North, M.; Pasquale, R., Mechanism of cyclic carbonate synthesis from epoxides and CO₂. *Angewandte Chemie* **2009**, 121 (16), 2990-2992.
8. Jiang, J.-L.; Gao, F.; Hua, R.; Qiu, X., Re (CO) 5Br-catalyzed coupling of epoxides with CO₂ affording cyclic carbonates under solvent-free conditions. *The Journal of organic chemistry* **2005**, 70 (1), 381-383.
9. Yasuda, H.; He, L.-N.; Sakakura, T., Cyclic carbonate synthesis from supercritical carbon dioxide and epoxide over lanthanide oxochloride. *Journal of Catalysis* **2002**, 209 (2), 547-550.
10. Whiteoak, C. J.; Nova, A.; Maseras, F.; Kleij, A. W., Merging sustainability with organocatalysis in the formation of organic carbonates by using CO₂ as a feedstock. *ChemSusChem* **2012**, 5 (10), 2032-2038.
11. Yoshida, Y.; Arai, Y.; Kado, S.; Kunimori, K.; Tomishige, K., Direct synthesis of organic carbonates from the reaction of CO₂ with methanol and ethanol over CeO₂ catalysts. *Catalysis today* **2006**, 115 (1-4), 95-101.
12. Polyzos, A.; O'Brien, M.; Petersen, T. P.; Baxendale, I. R.; Ley, S. V., The continuous - flow synthesis of carboxylic acids using CO₂ in a tube - in - tube gas permeable membrane reactor. *Angewandte Chemie International Edition* **2011**, 50 (5), 1190-1193.
13. Greenhalgh, M. D.; Thomas, S. P., Iron-catalyzed, highly regioselective synthesis of α -aryl carboxylic acids from styrene derivatives and CO₂. *Journal of the American Chemical Society* **2012**, 134 (29), 11900-11903.
14. Centi, G.; Perathoner, S., Opportunities and prospects in the chemical recycling of carbon dioxide to fuels. *Catalysis Today* **2009**, 148 (3-4), 191-205.
15. Bhanage, B. M.; Fujita, S.-i.; Ikushima, Y.; Arai, M., Synthesis of dimethyl carbonate and glycols from carbon dioxide, epoxides, and methanol using heterogeneous basic metal oxide catalysts with high activity and selectivity. *Applied Catalysis A: General* **2001**, 219 (1-2), 259-266.
16. Bhanage, B. M.; Fujita, S.-i.; Ikushima, Y.; Torii, K.; Arai, M., Synthesis of dimethyl carbonate and glycols from carbon dioxide, epoxides and methanol using heterogeneous Mg containing smectite catalysts: effect of reaction variables on activity and selectivity performance. *Green Chemistry* **2003**, 5 (1), 71-75.
17. Holtbruegge, J.; Leimbrink, M.; Lutze, P.; Górak, A., Synthesis of dimethyl carbonate and propylene glycol by transesterification of propylene carbonate with methanol: Catalyst screening, chemical equilibrium and reaction kinetics. *Chemical Engineering Science* **2013**, 104, 347-360.
18. Buysch, H.-J.; Krimm, H.; Rudolph, H., Process for the preparation of dialkyl carbonates. Google Patents: 1980.
19. Urano, Y.; Kirishiki, M.; Onda, Y.; Tsuneki, H., Process for preparing dialkyl carbonates. Google Patents: 1995.
20. Song, Z.; Jin, X.; Hu, Y.; Subramaniam, B.; Chaudhari, R. V., Intriguing Catalyst (CaO) Pretreatment Effects and Mechanistic Insights during Propylene Carbonate Transesterification with Methanol. *ACS Sustainable Chemistry & Engineering* **2017**, 5 (6), 4718-4729.
21. Pyrlík, A.; Hoelderich, W. F.; Müller, K.; Arlt, W.; Strautmman, J.; Kruse, D., Dimethyl carbonate via transesterification of propylene carbonate with methanol over ion exchange resins. *Applied Catalysis B: Environmental* **2012**, 125, 486-491.
22. Unnikrishnan, P.; Srinivas, D., Calcined, Rare Earth Modified Hydrotalcite as a Solid, Reusable Catalyst for Dimethyl Carbonate Synthesis. *Industrial & Engineering Chemistry Research* **2012**, 51 (18), 6356-6363.
23. Joseph, B. R., Method of making a polyether using a double metal cyanide complex

- compound. Google Patents: 1966.
24. Le-Khac, B., Double metal cyanide complex catalysts. Google Patents: 1995.
 25. Kruper Jr, W. J.; Swart, D. J., Carbon dioxide oxirane copolymers prepared using double metal cyanide complexes. Google Patents: 1985.
 26. Kuyper, J.; van Schaik-Struykenkamp, P., Process for the polymerization of epoxides. Google Patents: 1984.
 27. Jack, M., Method of making a polyether using a double metal cyanide complex compound. US3278457. Google Patents: 1966.
 28. Dienes, Y.; Leitner, W.; Müller, M. G.; Offermans, W. K.; Reier, T.; Reinholdt, A.; Weirich, T. E.; Müller, T. E., Hybrid Sol–Gel Double Metal Cyanide Catalysts For The Copolymerisation of Styrene Oxide And CO₂. *Green Chemistry* **2012**, *14* (4), 1168-1177.
 29. O'connor, J. M.; Lickei, D. L.; Grieve, R. L., Preparing polyether polyols with DMC catalysts. US6539101. 2002.
 30. Kim, I.; Ahn, J.-T.; Ha, C. S.; Yang, C. S.; Park, I., Polymerization of Propylene Oxide By Using Double Metal Cyanide Catalysts And The Application To Polyurethane Elastomer. *Polymer* **2003**, *44* (11), 3417-3428.
 31. Kim, I.; Ahn, J.-T.; Lee, S.-H.; Ha, C.-S.; Park, D.-W., Preparation of Multi-Metal Cyanide Catalysts And Ring-Opening Polymerization of Propylene Oxide. *Catalysis today* **2004**, *93*, 511-516.
 32. Kim, I.; Yi, M. J.; Lee, K. J.; Park, D.-W.; Kim, B. U.; Ha, C.-S., Aliphatic Polycarbonate Synthesis By Copolymerization of Carbon Dioxide With Epoxides Over Double Metal Cyanide Catalysts Prepared By Using ZnX₂ (X= F, Cl, Br, I). *Catalysis today* **2006**, *111* (3), 292-296.
 33. Eleveld, M. B., Grotenbreg, Robert Adrianus Wilhelmus, Van Kempen, Ronald Preparation of A Double Metal Cyanide Catalyst. US 6977236. 2005.
 34. Srinivas, D.; Srivastava, R.; Ratnasamy, P., Transesterification Catalyst And A Process For The Preparation Thereof. US 7754643. 2010.
 35. Srivastava, R.; Srinivas, D.; Ratnasamy, P., Fe–Zn Double-Metal Cyanide Complexes As Novel, Solid Transesterification Catalysts. *Journal of Catalysis* **2006**, *241* (1), 34-44.
 36. Murugan, C.; Bajaj, H., Transesterification of propylene carbonate with methanol using Mg–Al–CO₃ hydrotalcite as solid base catalyst. *Indian journal of chemistry. Section A, Inorganic, bio-inorganic, physical, theoretical & analytical chemistry* **2010**, *49* (9), 1182.
 37. Song, Z.; Subramaniam, B.; Chaudhari, R. V., Transesterification of Propylene Carbonate with Methanol Using Fe–Mn Double Metal Cyanide Catalyst. *ACS Sustainable Chemistry & Engineering* **2019**, *7* (6), 5698-5710.
 38. Ramachandran, P.; Chaudhari, R., *Three-phase Catalytic Reactors*. Gordon & Breach Science Pub: 1983; Vol. 2.
 39. Studio, A. V., Modeling, Optimization and Nonlinear Parameter Estimation for Scientists and Engineers. 2011.
 40. Bernacki, J. P.; Murphy, R. M., Model discrimination and mechanistic interpretation of kinetic data in protein aggregation studies. *Biophysical journal* **2009**, *96* (7), 2871-2887.
 41. Song, Z.; Subramaniam, B.; Chaudhari, R. V., Kinetic Study of CaO-Catalyzed Transesterification of Cyclic Carbonates with Methanol. *Industrial & Engineering Chemistry Research* **2018**, *57* (44), 14977-14987.
 42. Jin, X.; Bobba, P.; Reding, N.; Song, Z.; Thapa, P. S.; Prasad, G.; Subramaniam, B.; Chaudhari, R. V., Kinetic modeling of carboxylation of propylene oxide to propylene carbonate using ion-exchange resin catalyst in a semi-batch slurry reactor. *Chemical Engineering Science* **2017**, *168*, 189-203.
 43. Sirjean, B.; Glaude, P. A.; Ruizlopez, M. F.; Fournet, R., Theoretical Kinetic Study of the Ring Opening of Cyclic Alkanes. *Physics* **2009**.
 44. Kumar, A.; Some, D.; Kiriamiti, K. H. In *Pretreatment of CaO Catalyst for Transesterification of Croton Megalocarpus Oil*, Proceedings of Sustainable Research and Innovation Conference, 2014; pp 150-153.

45. Kouzu, M.; Kasuno, T.; Tajika, M.; Yamanaka, S.; Hidaka, J., Active phase of calcium oxide used as solid base catalyst for transesterification of soybean oil with refluxing methanol. *Applied Catalysis A: General* **2008**, *334* (1–2), 357-365.
46. Tanabe, K.; Misono, M.; Ono, Y.; Hattori, H.; Tanabe, K.; Misono, M.; Ono, Y.; Hattori, H., *New solid acids and bases studies in the surface science and catalysis*. Elsevier, Amsterdam: 1989.
47. Schuchardt, U.; Sercheli, R.; Vargas, R. M., Transesterification of vegetable oils: a review. *Journal of the Brazilian Chemical Society* **1998**, *9* (3), 199-210.
48. Gryglewicz, S., Rapeseed oil methyl esters preparation using heterogeneous catalysts. *Bioresource Technology* **1999**, *70* (3), 249-253.
49. Liu, X.; He, H.; Wang, Y.; Zhu, S., Transesterification of soybean oil to biodiesel using SrO as a solid base catalyst. *Catalysis Communications* **2007**, *8* (7), 1107-1111.
50. Kouzu, M.; Kasuno, T.; Tajika, M.; Sugimoto, Y.; Yamanaka, S.; Hidaka, J., Calcium oxide as a solid base catalyst for transesterification of soybean oil and its application to biodiesel production. *Fuel* **2008**, *87* (12), 2798-2806.
51. Masood, H.; Yunus, R.; Choong, T. S. Y.; Rashid, U.; Taufiq Yap, Y. H., Synthesis and characterization of calcium methoxide as heterogeneous catalyst for trimethylolpropane esters conversion reaction. *Applied Catalysis A: General* **2012**, *425–426*, 184-190.

Table of Contents

A kinetic model involves the activation sequence of reactants PC, methanol and intermediate provides the best description of the experimental data with respect to reaction parameters over a wide range of conditions.

Kinetic investigations clarify the specific activation sequence of methanol, propylene carbonate and monotransesterified product (2-HMC) to form dimethyl carbonate

